r-Regular Shape Reconstruction from Unorganized Points

Dominique Attali

Communication Technology Laboratory, Swiss Federal Institute of Technology ETH,
Gloriastr. 35, CH-8092 Zurich, Switzerland
E-mail: Dominique.Attali@vision.ee.ethz.ch

Abstract

In this paper, the problem of reconstructing a surface, given a set of scattered data points is addressed. First, a precise formulation of the reconstruction problem is proposed. The solution is mathematically defined as a particular mesh of the surface called the *normalized mesh*. This solution has the property to be included inside the Delaunay graph.

A criterion to select boundary faces inside the Delaunay graph is proposed. This criterion is proven to provide the exact solution in 2D for points sampling a r-regular shapes with a sampling path $\epsilon < 0.38r$. In $3D$, this results cannot be extended and the criterion cannot retrieve every faces. Some heuristics are then proposed in order to complete the surface.

1   Introduction

This paper addresses the problem of meshing a surface only known by an unorganized set of points. Such a problem may occur in many domains including pattern recognition, computer vision, and graphics. Meshing the boundary of an object is useful to study its geometry (volume, axes of inertia, area), to decide if a point is inside or outside the object, to provide a smooth interpolation of the boundary, or to display the object.

The initial data is a set of points with no structure, which sample a surface. Such points can be measured directly on the boundary of an object using 3D sensors or laser range scanning systems. They can also result from the segmentation of a 3D volumetric image. Starting from this mere set of points only known by their coordinates, we are interested in building a mesh induced by the proximity relationships of the points on the surface.

To solve this problem, it is common to compute first a neighbourhood graph of the data points and then to restrict the search for a mesh inside this neighbourhood graph. Many neighbourhood graphs for which efficient algorithms from computational geometry exist have been tried. In [1], the k-nearest neighbour graph is used to estimate a signed distance to the surface. After this step, a set of cubes crossing the surface is computed and a marching-cube algorithm provides the searched triangulation. Another appealing idea consists in starting from the convex hull of the points and to sculpture this convex hull until it passes through all the points [2]. The sculpture of the convex hull can be simplified by computing the Delaunay graph [3]. Thus, the sculpture consists in removing tetrahedra located on the current surface in such a way that at each step, the current surface remains a polyhedron. A drawback of such an approach is that no change of the topology is allowed and consequently, it is impossible to get a surface formed of several connected components or having holes. The Voronoi graph is sometimes used to get additional information on the skeleton of the object [4, 5, 6].

More complex graphs have also been introduced like α-hulls and α-shapes [7, 8]. α-shapes are a generalization of the convex hull of a point set. An α-shape is a polytope surrounding the set of points. The parameter α controls the maximum "curvature" of any cavity of the polytope. Several α-shapes with different values of α are presented in figure 1. The choice of the parameter α might be tricky.
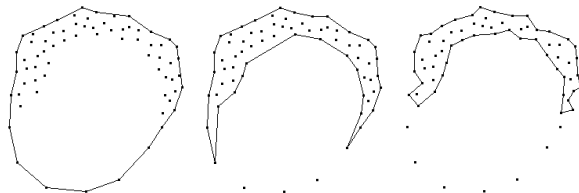

Figure 1: α-shapes

Although a large amount of work has been done on this topic, few theoretical results [9] exist mainly due to the difficulty formalizing the problem. In most papers, no mathematical definition of the searched mesh is given. In section 2, we try to fill this deficiency by formulating the problem more precisely. In particular, the searched solution is defined as a particular mesh of the surface called the *normalized mesh*. In section 3, a method is proposed to build this solution. The convergence of our approach is proven in the two-dimensional case for r-*regular shapes*. Unfortunately, the demonstration cannot be extended to the three-dimensional case. It results that some faces of the surface cannot be retrieved by our algorithm. In section 4, some heuristics are proposed to complete the surface.

2   Problem statement

In this section, definitions are given in three-dimensional space but they can easily be extended in a space of any dimension. d represents the Euclidean distance and $\overline{X}$ designates the closure of the set X.

2.1   General case

Let S be the unknown surface to mesh and E a finite set of points located on S. To measure the quality of the sample, we introduce the notion of sampling path:

Definition 1 (Sampling path) $E \subset S$ *is said to sample* S *with the sampling path* ϵ *if any sphere with radius* ϵ *and center in* S *contains at least one sample point in* E *(Fig. 2).*

The end of this section is concerned with building up a *normalized mesh* from certain elementary spaces called *cells*.
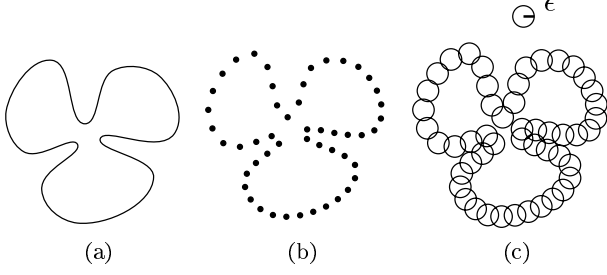
Figure 2: (a) Curve. (b) Sample of the curve with sampling path ϵ. (c) Disks containing the curve.

A cell is just a generalization to an arbitrary number of vertices of a simplex.

Definition 2 (cell) *A k-cell $[a_1, \cdots, a_k]$ is the set of points $\sum_{i=1}^{k} \lambda_i a_i$, where $a_1, \ldots, a_k$ are points, and the λ_i are real numbers such that $\lambda_i \geq 0$ for all i and $\sum_{i=1}^{k} \lambda_i = 1$. The points $a_1, \ldots, a_n$ are called the vertices of the cell.*

The normalized mesh is a particular mesh of the surface S defined as a union of cells with vertices at the data points E:

Definition 3 (Normalized mesh) *The normalized mesh of S associated to E is the set of cells $[p_1, \cdots, p_k]$ with $p_i \in E$ for which exists a point $m \in S$ such that $d(m, p_1) = \cdots = d(m, p_k) = d(m, E)$.*
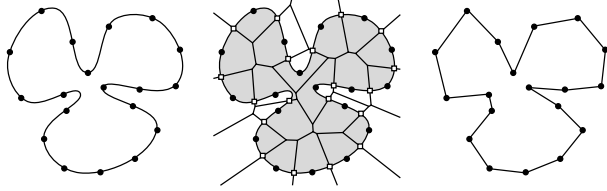

Figure 3: Construction of the normalized mesh from the Voronoi graph of the sample points.

By definition, the normalized mesh is included in the Delaunay diagram of E. It is formed of the Delaunay elements (edges, faces and simplices) whose dual intersects the surface (Fig. 3). Generally, the normalized mesh is formed of edges in $2D$ and triangular facets in $3D$ but it may also happen that the normalized mesh has a non-zero thickness if it includes a cell with not linearly independent vertices. One can remark that if E samples S with the sampling path ϵ, then each face of the normalized mesh has diameter lower than 2ϵ.

Normalized mesh are particularly attractive as they provides a piecewise linear interpolant of the surface that converges to the surface when the sampling path tends to 0:

Proposition 1 (Convergence) *Let S be a surface and E_n be a sample of S with sampling path $\frac{1}{n}$. Let S_n be the normalized interpolant of S associated to E_n. Then:*

$$\lim_{n \to \infty} S_n = \overline{S}$$

.

Using the previously defined notions, it is now possible to give a precise formulation of the initial reconstruction problem. Given a surface S and a set of points E located on S, the problem can be expressed as finding the normalized mesh of S associated to E. Such a mesh provides a natural solution. It is a piecewise linear interpolant of the surface which tends to S when the sampling path tends to 0.

2.2 r-regular shapes

In order to simplify the search for the normalized mesh, we will assume in the next section that S is the boundary of an r-regular shape.

Definition 4 (r-regular shape) *Let B_0 be the unit ball. A shape X is said to be r-regular if it is morphologically open and closed with respect to a disk of radius $r > 0$:*

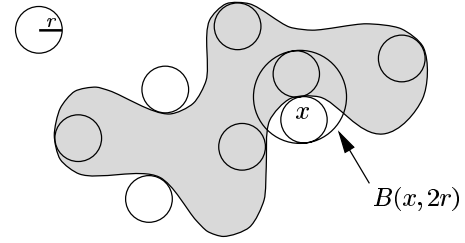$$X = (X \ominus rB_0) \oplus rB_0 = (X \oplus rB_0) \ominus rB_0$$

Figure 4: r-regular shape

The concept of r-regular shapes was first introduced in the field of mathematical morphology [10]. Since the parameter r can be arbitrarily small, r-regular shapes offer a relevant model to represent objects arising in image analysis [11]. r-regular shapes have many nice geometric properties (Fig. 4):

1. The boundary of an r-regular shape has at each point a tangent and a radius of curvature greater or equal to r.

2. The boundary of an r-regular shape divides any ball with radius $2r$ and center on the boundary in exactly two connected components.

3. From the previous property, it follows that if $\epsilon < 2r$, the normalized mesh provides a tiling of the surface. In other words, the normalized mesh retains all the topological properties of the surface.

4. In the two-dimensional space, any circle passing through three distinct boundary points has radius greater than r. This property will be crucial in the next section to validate our algorithm. Unfortunately, this property has no $3D$ equivalent.

3 Characterizing boundary faces

In this section, our goal is to characterize faces of the normalized mesh. From the previous section, we know that this search can be restricted inside the Delaunay diagram of the sample points. Therefore, the adressed problem is to determine which faces of the Delaunay diagram belong to the normalized mesh. Afterwards, a *Delaunay sphere* refers to a
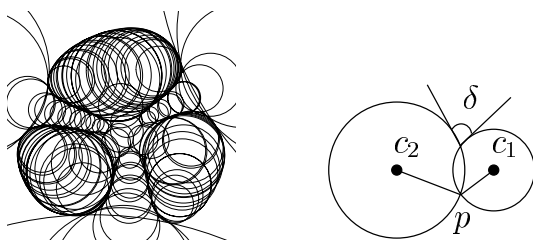
Figure 5: Angle formed by Delaunay disks

sphere circumscribed to a Delaunay simplex. The surface is assumed to be the boundary of an r-regular shape.

To detect boundary faces, one can take advantage of the following remark. In 2D, Delaunay discs tend to maximal discs of the object and of the complement of the object when the sampling density tends to 0 [12]. Consequently, Delaunay discs become tangent to the boundary (Fig. 5). In 3D, to evaluate the belonging of a Delaunay triangle to the surface, we are going to measure the angle formed by the two Delaunay spheres passing on both sides of this triangle. More precisely, if T is a Delaunay triangle, c_1 and c_2 the centers of the two Delaunay spheres passing through T and p a vertex of T, we define (Fig. 5):

$$\delta(T) = \pi - \widehat{c_1 p c_2}$$

Broadly speaking, when the angle $\delta(T)$ is near 0, there is every chance that the triangle T belongs to the boundary. On the contrary, if this angle is near π, the triangle has every chance to be inside or outside the object.

Let us remark that an analogous criterion was proposed in [3]. The distance from a face T to the Delaunay sphere passing through T was used in order to measure the belonging of this face to the surface. One advantage of our criterion is to be symmetric with respect to the boundary.

To reconstruct the surface, we are going to consider the set of triangles T for which $\delta(T) \leq \delta_0$. This set is called afterwards S_{δ_0}.

3.1   2D case

In 2D, S_{δ_0} is a set of edges selected from the Delaunay diagram of E. The main result of this paper is that if $\epsilon < \sin(\frac{\pi}{8})r$, then the set of edges $S_{\frac{\pi}{2}}$ is the normalized mesh of S associated to the points E. To demonstrate this result, one has first to establish the following proposition:

Proposition 2 *Let X be an r-regular shape and E be a sample of ∂X with sampling path ϵ. For each edge (pq) of the Delaunay diagram of E, we have :*

1. *if (pq) belongs to the normalized mesh and $\epsilon < \frac{r}{2}$, then $\delta(pq) < \frac{\pi}{2}$*

2. *if (pq) does not belong to the normalized mesh and $\epsilon < \sin(\frac{\pi}{8})r$, then $\delta(pq) > \frac{\pi}{2}$*

Proof. A complete proof may be found in [13]. In this paper, we only demonstrate the first point of the proposition. The second point can be established in a similar way.

Let (pq) be an edge of the normalized mesh (Fig. 6). Let $B(x_1, r_1)$ and $B(x_2, r_2)$ be the two Delaunay disks intersecting at points p and q. If m designates the middle point of

$[pq]$, we have :

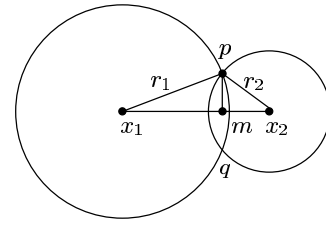$$\delta = \pi - \widehat{x_1 p m} - \widehat{m p x_2}$$

Figure 6: Illustration of the proof.

A disk intersecting the boundary of an r-regular shape in 3 distinct points has radius greater than r. Consequently, $r_1 \geq r$ and $r_2 \geq r$. Furthermore, edges of the normalized mesh have length smaller than 2ϵ. It follows that $d(p, m) < \epsilon$. Thus :

$$\cos(\widehat{x_1 p m}) = \frac{d(p, m)}{r_1} < \frac{\epsilon}{r} < \frac{1}{2}$$

$$\cos(\widehat{m p x_2}) = \frac{d(p, m)}{r_2} < \frac{\epsilon}{r} < \frac{1}{2}$$

Consequently, $\widehat{x_1 p m} > \frac{\pi}{3}$, $\widehat{m p x_2} > \frac{\pi}{3}$ and $\delta < \frac{\pi}{3} < \frac{\pi}{2}$.

Proposition 3 *Let X be an r-regular shape and E be a sample of ∂X with sampling path ϵ. If $\epsilon < \sin(\frac{\pi}{8})r$, then $S_{\frac{\pi}{2}}$ is the normalized mesh*
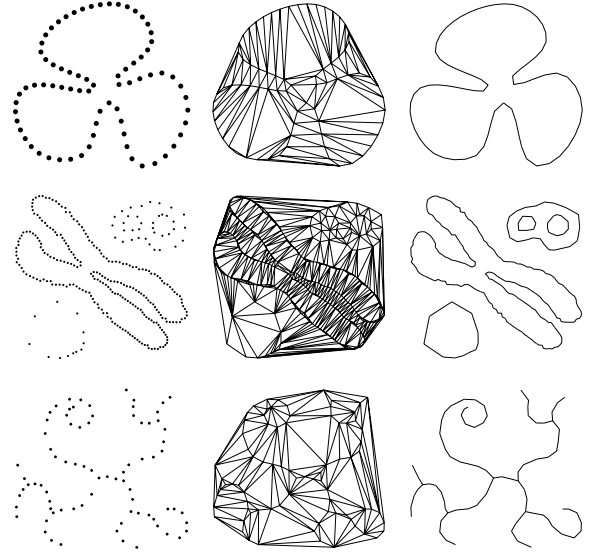

Figure 7: Sample points, Delaunay triangles and normalized mesh.

The beauty of this result lies in the fact that there is no need to know the two parameters r and ϵ in order to compute the normalized mesh. Moreover, the sampling path has no need to be close to zero in order to find the correct result. It is enough that the sampling path ϵ and the constant r characterizing the searched shape have approximately the same

order. The computational time is also very attractive. The detection of boundary faces requires only the computation of a Voronoi graph. Given n sample points in a N-dimensional space, the computational time is $O(n \log n + n^{\lceil N/2 \rceil})$. Figure 7 illustrates the robustness of the proposed method on several examples. The method was able to detect curves even if not closed and even when the points were not regularly spaced on the curves.
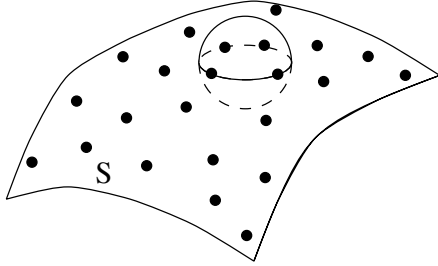
3.2   3D case

Figure 8: In 3D, a Delaunay sphere may intersect the surface

In $3D$, contrary to the 2D case, it may happen that some Delaunay spheres intersect the boundary without being tangent to it as illustrated in figure 8. This new phenomenon makes it impossible to minorate the radius of the Delaunay spheres. Consequently, proposition 2 cannot be generalized.
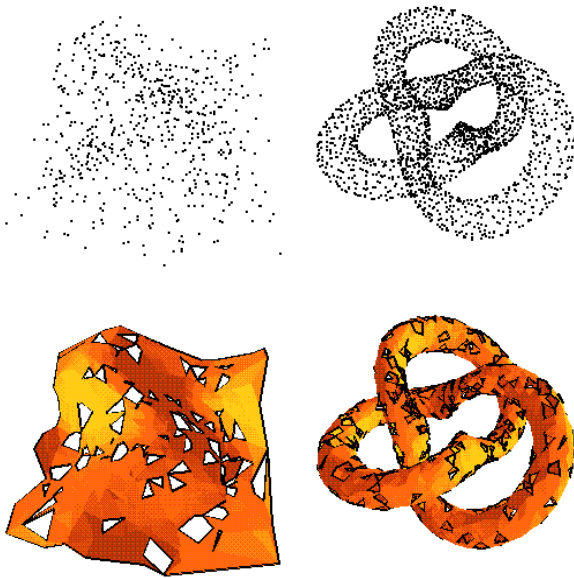

Figure 9: Some boundary faces are missing.

Experimentally, one can remark that the set $S_{\frac{\pi}{2}}$ does not capture all faces of the normalized mesh (Fig. 9). Some triangles are missing and the surface has more or less holes, depending on the distribution of sample points (Fig. 10). Nevertheless, as the proposed criterion does not produce erroneous triangles, one can start from this first approximation of the surface in order to find the solution.
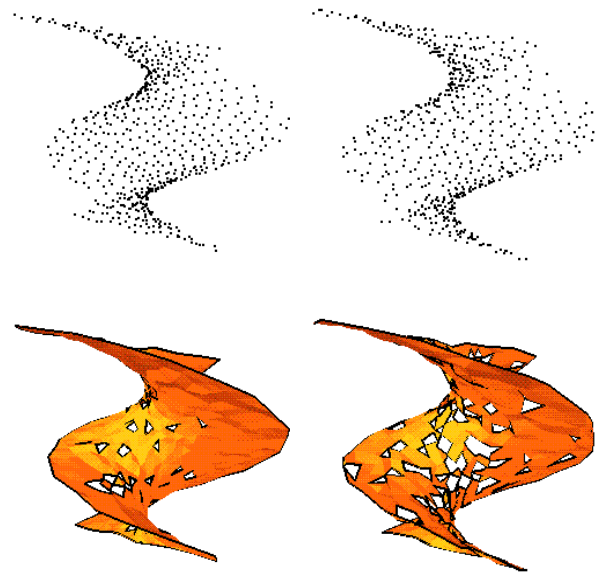

Figure 10: The number of missing triangles depends on the distribution of sample points.

4   Closing the surface

In this section, two different heuristics are proposed in order to complete surfaces from the previous section. Afterwards, the term "surface" refers to the set $S_{\frac{\pi}{2}}$.

4.1   Triangulation of the border

The border of the surface is formed of polygons. A first idea is to triangulate each polygon of the border independently from the others (Fig. 17). Given a simple polygon on the border of the surface, a triangulation of this polygon can be performed by adding one after the other Delaunay triangles sharing two or three edges with this polygon. If the triangulation fails, the surface cannot be closed by this method. Border polygons that are not simple must first be splitted up.

This approach has the advantage to make absolutely no assumption on the distribution of sample points. It deals with closed as well as open surfaces. Nevertheless, as illustrated on figure 11, it may sometimes not provide the expected solution. This approach has not yet been implemented.
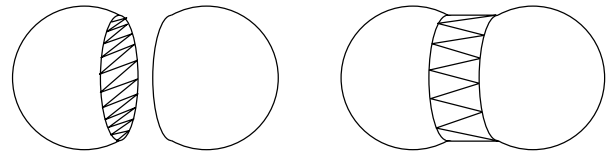

Figure 11: Two possible triangulations of the border.

4.2   Tessellation of the volume

In this section, a volume-based approach is proposed. Instead of computing directly the surface, we first try to find a

collection of objects whose boundary provides the searched surface. This approach assumes surfaces to be closed, and consequently, is less general than the previous one.
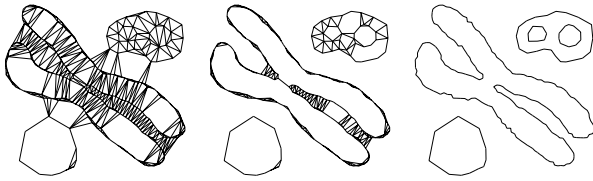

Figure 12: Illustration of the algorithm in 2D.

The main idea is to merge Delaunay tetrahedra until space is partitionned into a satisfactory number of objects. Our algorithm aggregates Delaunay tetrahedra as follows :

1. INITIALIZATION. Delaunay tetrahedra and the complement of the convex hull of the sample points form the initial set of objects. Delaunay triangles are put in a list $\mathcal{L}$ that is sorted according to the diameter of triangles.

2. MERGE. While $\mathcal{L}$ is not empty, the triangle T having greatest diameter is taken out from $\mathcal{L}$. If T separates two different objects O_1 and O_2, those two objects are merged providing that :

   - no triangle from $S_{\frac{\pi}{2}}$ disappears,

   - the merge does not isolate sample points inside $O_1 \cup O_2$. In other words, after the merge, every sample point must still belong to the boundary of at least one object (Fig. 13).
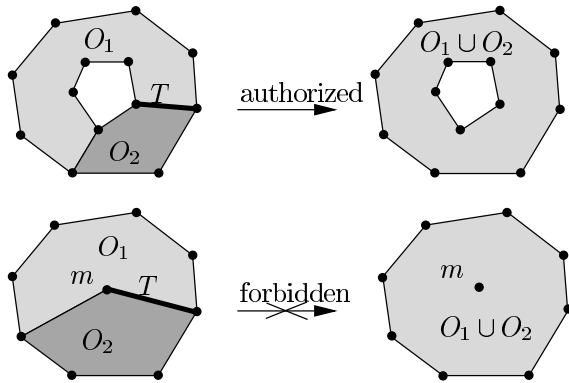

Figure 13: Rules to merge objects.

As soon as two objects share an important number of boundary triangles, they cannot merge anymore. Rules chosen to merge tetrahedra differ from rules used in [3] to sculpture the convex hull. In particular, more operations are permitted in order to allow topological change of the surface. The result is a set of closed surfaces of arbitrary topology.

If n designates the number of sample points and k the number of Delaunay faces in the list at the beginning of the algorithm, the complexity is $O(k \log k + kn^2)$. Indeed, the sort is in $O(k \log k)$. To detect a possible merge between two objects, it is necessary to consider the neighbours of each sample point, which can be n in the worst case. Consequently, the complexity of the algorithm is $O(n^3)$ in 2D and $O(n^4)$ in 3D.

Figure 14 presents some results. The number of objects detected by our algorithm remains small. The percentage of tetrahedra not belonging to the main components is less than 0.5%.
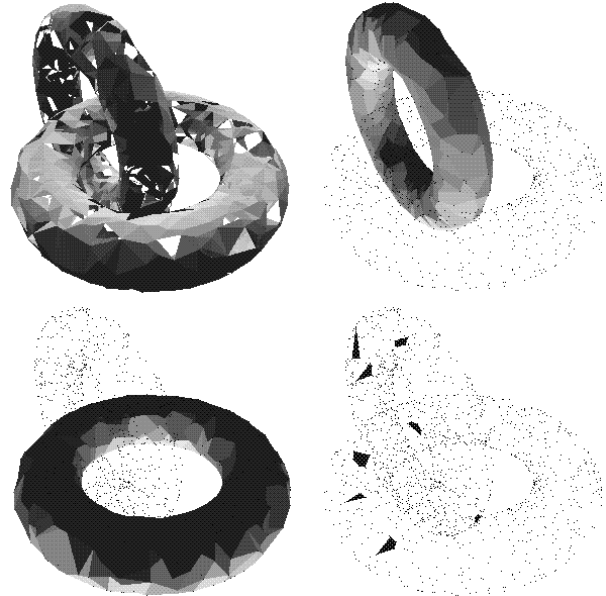

Figure 14: Uncomplete surface from the previous section. First, second and other components resulting from the merge of Delaunay tetrahedra.
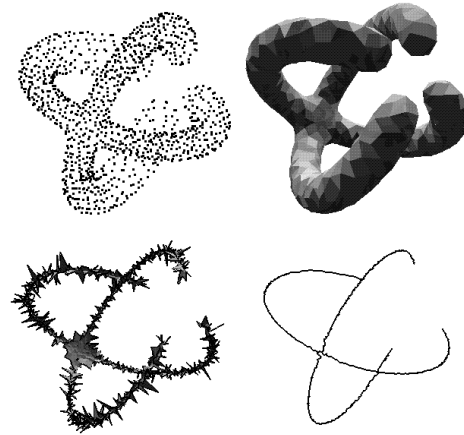

Figure 15: Sample points, reconstructed object, initial and simplified skeleton.

One advantage of this approach is that the skeleton of objects can easily be deduced (Fig. 15). The skeleton is a very famous representation of objects from image analysis and computer vision. It is a thin figure which retains all the topological properties of the object. It is useful to

describe and analyse objects. In 3D, it is made up of surfaces and curves passing through the middle of the object. The skeleton can be computed by considering the dual of the Delaunay tetrahedra included in the object.

5 Conclusion

In this paper, a precise formulation of the reconstruction problem has been given. We defined the solution as a particular subset of the Delaunay diagram. A first method has been proposed to construct this solution. The convergence of this method has been established in 2D. For 3D objects, the method does not detect every boundary face. Two methods have been proposed for completing surfaces and detect missing faces.

A weak point of our study is that points must be located on or near the boundary of the objects. In the case of real data, this assumption cannot always be fulfilled. Sample points may form a dense cluster around the objects. A new formulation of the reconstruction problem must then be proposed. Current research is directed towards this direction. An idea would be to combine α-shapes and the set of boundary faces detected with the criterion δ (Fig. 16). Indeed, the two approaches seem to complement one another. While α-shapes can capture noisy set of points, our approach enables to connect points located on curves and surfaces.
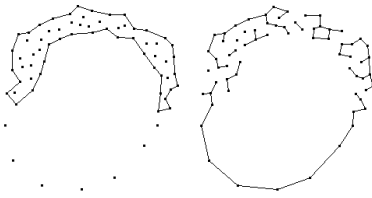

Figure 16: comparison of α-shape and $S_{\frac{\pi}{2}}$.

References

[1] H. Hoppe, T. DeRose, T. Duchamp, J. McDonnald, and W. Stuetzle. Surface reconstruction from unorganized points. *SIGGRAPH'92, Computer Graphics*, 26(2):71–77, 1992.

[2] J. O'Rourke. Polyhedra of minimal area as 3d objects models. In *Proc. of the International Joint Conference on Artificial Intelligence*, pages 664–666, 1981.

[3] J. D. Boissonnat. Geometric structures for three-dimensional shape representation. *ACM Transactions on Graphics*, 3(4):266–286, October 1984.

[4] J. Fairfield. Segmenting dot patterns by voronoi diagram concavity. *IEEE Trans. on PAMI*, 5(1):104–110, 1983.

[5] J. O'Rourke, H. Booth, and R. Washington. Connect-the-dots: A new heuristic. *Computer Vision, Graphics and Image Processing*, 39:258–266, 1987.

[6] A. C. F. Colchester, G. P. Robinson, and L. D. Griffin. A unified approach to the segmentation of grey-level and dot-pattern. In *Proc. of the 11th International Conference on Pattern Recognition*, pages 319–322, The Netherlands, 1992.

[7] H. Edelsbrunner, D. G. Kirkpatrick, and R. Seidel. On the shape of a set of points in the plane. *IEEE Transactions on Information Theory*, 29(4):551–559, 1983.

[8] H. Edelsbrunner and E. P. Mucke. Three-dimensional alpha shapes. *ACM Transactions on Graphics*, 13(1):43–72, 1994.

[9] S. Rippa. Minimal roughness property of the delaunay triangulation. *Computer Aided Geometric Design*, 7:489–497, 1990.

[10] J. Serra. *Image Analysis and Mathematical Morphology*. Academic Press, London, 1982.

[11] J. W. Brandt and V. R. Algazi. Continuous skeleton computation by Voronoi diagram. *CVGIP: Image Understanding*, 55(3):329–337, 1992.

[12] J. W. Brandt. Convergence and continuity criteria for discrete approximations of the continuous planar skeletons. *CVGIP : Image Understanding*, 59(1):116–124, 1994.

[13] D. Attali. *Squelettes et graphes de Vorono 2D et 3D*. PhD thesis, Universit Joseph Fourier- Grenoble I, October 1995.
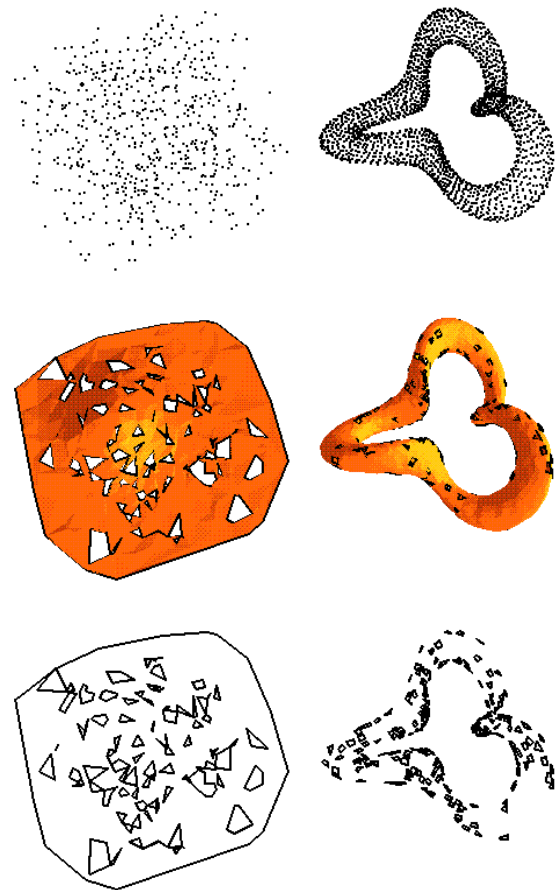
Figure 17: Sample points, reconstructed surface and border of the surface.